In vitro and in vivo characteristics of core shell type nanogel particles: Optimization of core cross-linking density and surface poly(ethylene glycol) density in PEGylated nanogels

In Vitro and *In Vivo* Characteristics of Core–Shell-Type Nanogel Particles: Optimization of Core Cross-Linking Density and Surface PEG Density in PEGylated Nanogels

Masato Tamura[1], Satoshi Ichinohe[2], Atsushi Tamura[2], Yutaka Ikeda[2,3,4],
and Yukio Nagasaki[1,2,3,4,5,*]

[1]*Graduate School of Comprehensive Human Sciences, University of Tsukuba, 1-1-1 Ten-noudai, Tsukuba, Ibaraki 305-8573, Japan*

[2]*Graduate School of Pure and Applied Sciences, University of Tsukuba, 1-1-1 Ten-noudai, Tsukuba, Ibaraki 305-8573, Japan*

[3]*Tsukuba Research Center for Interdisciplinary Materials Science (TIMS), University of Tsukuba, 1-1-1 Ten-noudai, Tsukuba, Ibaraki 305-8573, Japan*

[4]*Center for Tsukuba Advanced Research Alliance (TARA), University of Tsukuba, 1-1-1 Ten-noudai, Tsukuba, Ibaraki 305-8573, Japan*

[5]*International Center for Materials Nanoarchitectonics Satellite (MANA), National Institute for Materials Science (NIMS) and University of Tsukuba 1-1-1 Ten-noudai, Tsukuba, Ibaraki 305-8573, Japan*

* Corresponding author. Prof. Yukio Nagasaki (Tel: +81-29-853-5749. Fax: +81-29-853-5749. E-mail: yukio@nagalabo.jp).

Abstract

The biocompatibility and body distribution of PEGylated polyamine nanogels (composed of chemically cross-linked poly[2-*N,N*-(diethylamino)ethyl methacrylate] (PEAMA) gel cores surrounded by poly(ethylene glycol) (PEG) chains were investigated to evaluate their feasibility as drug nanocarriers for systemic administration. PEGylated nanogels with different cross-linking densities (1, 2, and 5 mol%) were prepared to evaluate their biocompatibilities by *in vitro* cytotoxicity assay, hemolysis assay, and *in vivo* acute toxicity. The toxic effect of the PEGylated nanogels derived from polyamine gel cores was significantly reduced when the cross-linking density was increased, and those with a cross-linking density of 5 mol% showed remarkably high median lethal dose (LD_{50}) values >200 mg/kg, despite the abundance of amino groups in the core. One hour after intravenous (i.v.) injection, the PEGylated nanogels were found to have been eliminated from systemic circulation, and less than 1% of the injected dose (I.D.) remained in the bloodstream. To improve the blood circulation time by increasing the surface PEG density of the PEGylated nanogels, post-PEGylation of the PEGylated nanogels (through the Menschutkin reaction between the tertiary amines of the PEAMA gel core and bromobenzyl-terminated short PEG) was carried out. The biodistribution study of these post-PEGylated nanogels revealed that the blood circulation time of the nanogels was definitely prolonged as the PEG content was increased. Therefore, the precise design of PEGylated nanogels, with increased cross-linking densities in their polyamine gel cores and increased surface PEG densities, seems promising for systemic applications.

Keywords

Introduction

Drug delivery systems (DDSs) have attracted much attention in the field of cancer chemotherapy because of their capability for improving quality of life (QOL) by reducing the severity of the side effects of drugs while increasing their therapeutic efficacy. In this regard, precisely constructed drug nanocarriers, including polymeric micelles, stealth liposomes, and other nanoparticles, have been developed to increase accumulation in the target tissue and release the encapsulated drugs there [1-3]. The surface modification of these drug carriers with poly(ethylene glycol) chains (PEGylation) represents an essential strategy for reducing nonspecific interactions with serum proteins and endotheliums in the blood stream, as well as avoiding recognition by immune systems such as the reticuloendothelial system (RES) [4-6]. Thus, stabilized nanocarriers tend to show long blood circulation times and facilitate accumulation in the tumor tissue through the effects of enhanced permeability and retention (EPR) [7]. In addition, external-stimuli-sensitive smart drug carriers that can release encapsulated drugs selectively in response to specific environments such as tumor extracellular acidic pH and enzymes have been developed to enhance the therapeutic efficacy in the targeted tissue [8-10]. Representative nanocarriers such as polymeric micelles and liposomes are prepared through the self-assembly of amphiphilic molecules in aqueous media [11, 12]. Pharmacokinetics of nanoparticles has been investigated mainly by labeling with fluorescent dyes or radionuclides of these amphiphiles. However, because a part of self-assembled nanocarriers may disintegrate during circulation *in vivo*, it is not easy to determine precise pharmacokinetics of intact nanoparticle itself. From the view point of pharmacokinetics study of nanoparticles themselves, nanoparticle without disintegration character might need to be further investigated.

We have reported core-shell-type PEGylated nanogels composed of chemically cross-linked poly[2-*N*,*N*-(diethylamino)ethyl methacrylate] (PEAMA) gel cores surrounded by PEG palisade layers [13-18]. Because of their chemically cross-linked polyamine gel core, the PEGylated nanogels show high stability against extremely dilute and high-salt conditions, in contrast to self-assembled nanocarriers. Moreover, the nanogels show pH-dependent swelling/deswelling transitions across the

pK_a of the PEAMA gel core around pH = 7.0 [13,14]; in other words, the nanogels swell in acidic conditions due to the increased osmotic pressure in addition to the electrostatic repulsion of the protonated PEAMA, and they deswell in alkaline conditions because of the hydrophobic interactions of the deprotonated PEAMA. In synchronization with this pH-dependent volume phase transition of such PEGylated nanogels, anti-tumor drugs incorporated in the core can be released in response to an acidic environment [15]. This polyamine gel core of the nanogels also acts as a reservoir of therapeutic molecules, including gold nanoparticles [16] and small interfering RNAs (siRNAs) [17,18], through coordination or electrostatic interactions. Although these PEGylated nanogels showed notable therapeutic effect under *in vitro* conditions, their *in vivo* performance has not yet been demonstrated. Therefore, *in vivo* studies of PEGylated nanogels are needed in order to investigate their possible use in clinical applications.

In this study, the fundamental *in vivo* behavior of PEGylated nanogels, including their biocompatibility and biodistribution after systemic administration, was evaluated. Biocompatibility studies of the PEGylated nanogels, including evaluation of their metabolic activities, hemolytic activities, and acute toxicities, were performed to investigate the relationship between the cross-linking density of the polyamine gel core and the toxic effect of the nanogel. Biodistribution studies of PEGylated nanogels intravenously administered to mice were performed using [^{125}I]-labeled PEGylated nanogels. We believe that the optimization of both the "core" and "shell" structures of such nanogels might be of significant importance for the development of cancer therapy using PEGylated nanogels as well as the development of nanocarriers.

2. Materials and Methods

2-1. Materials

α-Methoxy-ω-4-vinylbenzyl-PEG (MeO-PEG-VB) and α-acetal-ω-4-vinylbenzyl-PEG (acetal-PEG-VB) macromonomers were synthesized by ring-opening anionic polymerization of ethylene oxide according to previously described methods [16,17]. The number-averaged molecular weight (M_n) and polydispersity index (M_w/M_n) of MeO-PEG-VB were 9,500 and 1.05, and those of acetal-PEG-VB were 10,300 and 1.05, respectively; these were determined by size exclusion chromatography using the PEG standard (column: TSKgel G4000HR and TSKgel G3000HR; eluent: THF). 2-(N,N-Diethylamino)ethyl methacrylate (EAMA; Wako Pure Chemical Industries, Ltd., Osaka, Japan) and ethylene glycol dimethacrylate (EGDMA; Kanto Chemicals Co., Ltd., Tokyo, Japan) were dried over calcium hydride and distilled under reduced pressure. Potassium persulfate (KPS; Kanto Chemicals Co., Ltd.) was recrystallized from distilled water and dried under reduced pressure. Tetrahydrofuran (THF; Kanto Chemicals Co., Ltd.) was purified by Glass Contour Solvent dispensing system (Nikko Hansen & Co., Ltd., Osaka, Japan). p-(1-Ethoxyethoxy)styrene (PEES) was kindly provided by Tosoh (Tokyo, Japan) and was dried over calcium hydride and distilled under reduced pressure. Methyl iodide (CH_3I), sodium hydride (NaH), α,α′-dibromo-p-xylene and 4-[3-(2-methoxy-4-nitrophenyl)-2-(4-nitrophenyl)-2H-5-tetrazolio]-1,3-benzene disulfonate sodium salt (WST-8) (Dojindo, Kumamoto, Japan) were used without further purification.

2-2. Synthesis of nanogels by emulsion polymerization

PEGylated nanogels with different cross-linking densities (1, 2, and 5 mol%) were synthesized by emulsion copolymerization by varying the feed EGDMA concentration [13-18]. The typical synthetic method for PEGylated nanogels with a cross-linking density of 1 mol% was as follows: acetal-PEG-VB (500 mg, 48.5 μmol) and KPS (15.3 mg, 567 μmol) were loaded into a round-bottomed flask equipped with a three-way stopcock, and three vacuum and nitrogen purging cycles were carried out. EGDMA

(53.1 μL, 270 μmol) and water (20.3 mL) were then added to the flask. Since pH of the solution was around 8.0, the almost of all monomers were deprotonated under the present conditions. Emulsion polymerization was carried out by adding EAMA (1.09 mL, 5.40 mmol), and the reaction mixture was stirred for 24 h at room temperature under a nitrogen atmosphere. Purification was carried out by ultrafiltration (molecular weight cutoff (MWCO) of 200,000) in which methanol was used to remove the unreacted starting reagents, and this was followed by ultrafiltration using deionized, distilled water to replace the solvent. The obtained nanogel solution was used as a stock solution, the concentration of which was determined by weighing before and after lyophilization.

2-3. Synthesis of PEGylated nanogel bearing vinylphenol moiety and radiolabeling with [^{125}I]

A PEGylated nanogel bearing vinylphenol moieties, acted as radioisotope (RI) labeling sites, in its core (VP-nanogel) was synthesized using the above mentioned emulsion polymerization procedure. MeO-PEG-VB (1.0 g, 106 μmol), KPS (30.9 mg, 114 μmol), EGDMA (119 μL, 545 μmol), and EAMA (2.17 mL, 10.8 mmol) were reacted in this emulsion polymerization process in the presence *p*-(1-ethoxyethoxy)styrene (PEES) (105 μL, 541 μmol), which was used as a precursor for *p*-vinylphenol. The purification was carried out according to the abovementioned procedure. For the conversion of the PEES to phenol groups, the PEES-containing nanogel solution was hydrolyzed by adjusting pH to 2.0 with 0.1 mol L^{-1} HCl and stirring for 2 h at room temperature. After the reaction, the nanogel solution was neutralized with 0.1 mol L^{-1} NaOH, and then subjected to dialysis against distilled water (MWCO = 3,500) for 24 h to obtain the VP-nanogels. In this reaction, MeO-PEG-VB was used for the preparation of the nanogel instead of acetal-PEG-VB in order to avoid the hydrolysis of the acetal groups and undesirable side reactions in the process of PEES hydrolysis.

Radioiodination of the VP-nanogels was carried out using the chloramine-T method [19, 20]. Briefly, Na[^{125}I] solution (2 μL, 148 kBq, Perkin Elmer) and chloramine-T (2.5 mg/mL, 90 μL, 0.9 μmol) were mixed with the VP-nanogel solution (10 mg/mL, 2 mg). After 10 min of reaction at room

temperature, an excess of sodium persulfate (9.5 mg/ml, 200 µL, 8 µmol) was added to stop the reaction, and the mixture was passed through a gel filtration column (PD-10 column, GE Healthcare, eluent: 10 mM phosphate buffer with 150 mM NaCl, pH 7.4) to remove unreacted Na[125I] and the starting reagents. Each 500 µL fraction was collected and its radioactivity measured by a γ-counter (ARC-380, Aloka, Tokyo, Japan) to confirm the [125I]-labeling of the VP-nanogel. The specific radioactivity of the [125I]-labeled VP-nanogel was determined to be 1120 kcpm/mg. The obtained [125I]-labeled VP-nanogel solutions were diluted with phosphate buffered saline (PBS) to adjust the radioactivity to 1.0 Mcpm/mL, and they were used for the *in vivo* body distribution studies.

2-4. Synthesis of α-methoxy-ω-bromobenzyl-PEG and post-PEGylation of nanogel

The installation of the bromobenzyl moiety at the ω-end of PEG was carried out with α,α′-dibromo-*p*-xylene according to a previously described method [21]. Briefly, MeO-PEG-OH ($M_n = 480$, $M_w/M_n = 1.07$, 480 mg, 1.0 mmol) was dissolved in THF (60 mL), and this was followed by successive addition of NaH (36 mg, 1.5 mmol), NaI (150 mg, 1.0 mmol), and α,α′-dibromo-*p*-xylene (2.6 g, 10 mmol). The reaction mixture was stirred for 96 h at room temperature under light shielding. After passing through a plug of celite, the low-molecular-weight starting reagents were removed by silica gel column chromatography. The purified polymer was dissolved in 1,4-dioxane and then lyophilized to obtain α-methoxy-ω-bromobenzyl-PEG (MeO-PEG-Bz-Br) as an oil (98.2% yield). The structure of the obtained MeO-PEG-Bz-Br was determined by 1H NMR (Avance 500 MHz NMR, Bruker, Supporting information, Figure S1).

The quaternization reaction of the tertiary amino groups in the core of the VP-nanogel was performed according to a previously described method with slight modifications [18, 22]. Aqueous solutions of VP-nanogels (2 mL, 50 mg/mL) were diluted fourfold with acetonitrile, and subsequently, MeO-PEG-Bz-Br was added (0.89 mmol or 8.9 mmol: 0.5 or 5.0 molar equivalents against amino groups). The mixture was reacted for 72 h at room temperature. After the reaction, the obtained

nanogel solutions were purified by ultrafiltration (MWCO = 200,000) as described above. Model quaternized polyamine nanogel (QNG) was synthesized under the similar conditions to that of post-PEGylated nanogel using methyl iodide instead of MeO-PEG-Bz-Br. Briefly, VP-nanogels solution (100 mg, 1.78 mmol of tertiary amino groups) was dialyzed against 500 mL of methanol (dialysate was changed 4 times after 3 h, 6 h, 12 h and 24 h) to convert the solvent. After the solvent was completely converted to methanol, CH_3I was added to the solution (5.33 mmol: 3 molar equivalents against amino groups). The mixture was reacted for 48 h at room temperature. After the reaction, the obtained QNG solutions were purified by ultrafiltration (MWCO = 200,000), the procedure of which was similar to that of post-PEGylated nanogels.   The extent of substitution (ES) of EAMA with MeO-PEG-Bz-Br or CH_3I was determined by quantifying the residual EAMA by potentiometric titration using an automatic titrator (Mettler DL-25, Mettler-Toledo, Greifensee, Switzerland), according to a previously described method [22].

2-5. Size and ζ-potential measurements

Nanogels showed phase transition at around pH = 7, reflecting the pK_a of PEAMA in physiological condition (pK_a = 7.1) [18], and more than 95% of amino group in the core were protonated at pH = 5.5 [18]. In addition, pH in lysosome is reported to become less than 6.0 [15]. Thus, we have chosen pH = 5.5 to characterize nanogel under acidic conditions. The size of the nanogel was evaluated by dynamic light scattering (DLS) on a Zetasizer Nano ZS (Malvern Instruments, Ltd., U.K.) equipped with a 4 mW He-Ne ion laser (λ = 633 nm). The DLS measurements were carried out at 37.0 °C at a detection angle of 173° in 10 mM phosphate buffer solution containing 150 mM NaCl at pH 5.5 or 7.4. The obtained correlation functions were analyzed by the cumulant method to determine the hydrodynamic diameters and polydispersity indices (μ_2/Γ^2).

Measurements of the ζ-potential of the nanogels were performed on a Zetasizer Nano ZS. The measurements were carried out at 37.0 °C in 10 mM phosphate buffer solution at pH = 5.5 or 7.4.

2-6. Cytotoxicity studies

Colon-26 cells, derived from murine rectum carcinoma, were seeded at a density of 1×10^4 cells/well in a 96-well plate and incubated overnight at 37 °C in a 5% CO_2 humidified atmosphere. The nanogel was added at a concentration in the range 0.1 to 1.0 mg/mL, and the cells were incubated at 37 °C for 24 h. Then, 10 μL of WST-8 reagent [23] was added to each well, and the cells were incubated for a further 1 h at 37 °C. The absorbance at 450 nm of the formazan produced by living cells was measured using a microplate reader (Varioskan; Thermo Electron Co., Waltham, MA). The cell viability was calculated relative to the untreated cells.

2-7. Hemolysis test

Whole blood was collected from ICR mice (Charles River, Yokohama, Japan), and was centrifuged at 3000 rpm for 5 min to isolate the red blood cells (RBCs), which were then washed three times with cold PBS. The nanogel solutions (975 μL) were added to RBC solution (25 μL; 4×10^8 cells/mL), and incubated for 60 min at 37 °C with shaking at 300 rpm. After the incubation, intact RBCs were separated by centrifugation (3000 rpm for 5 min) and 100 μL of supernatant was collected. The amount of hemoglobin release was determined by reading the absorbance at 540 nm on a Varioskan microplate reader. To determine 100% hemolysis, RBCs were lysed with 1% Triton-X, and the hemolytic activity of the nanogels was calculated relative to the Triton-X. Less than 10% hemolysis was regarded as a nontoxic level in our experiments [24].

2-8. Median lethal dose (LD$_{50}$) in acute toxicity study

For the animal experiments, all procedures and animal care were approved by the Committee on the Ethics of Animal Experimentation of the University of Tsukuba and were conducted according to

the Guidelines for Animal Experimentation of the University of Tsukuba. Four-week-old male ICR mice (Crlj: CD1 mice) were purchased from Charles River, Japan. The LD_{50} values of the nanogels were determined by intravenous injection of the nanogel solutions into the ICR mice. The nanogel doses were elevated to 20, 50, 100, and 200 mg/kg of the mouse body weight. The experiments were carried out on 5–8 mice for each group.

2-9. Blood circulation and tissue distribution of nanogel

The [^{125}I]-labeled nanogel (200 μL, 200 kcpm) was injected into the tail veins of four-week-old ICR mice. After a prescribed time period, the mice were anesthetized with diethyl ether. Blood was then collected via cardiac puncture, and this was followed by perfusion with 10 mL of saline. Afterward, the major organs (heart, lung, liver, kidney, and spleen) were collected and their radioactivities were measured using a γ-counter (ARC380). The data were normalized with the radioactivity of the injected dose.

3. Results and Discussion

3-1. Synthesis and characterization of PEGylated nanogels with different cross-linking densities

The biocompatibility of drug carriers is a major concern for clinical applications. Therefore, the toxic effects of the PEGylated nanogels were evaluated in terms of their cytotoxicity, hemolytic activity, and *in vivo* acute toxicity. Previously, it was revealed that the cytotoxicity of PEGylated nanogels is largely dependent on the cross-linking density of the polyamine core, and the PEGylated nanogel with a cross-linking density of 1 mol% showed lower cytotoxicity than that with 0.1 mol% cross-linking density [25]. In this study, the cross-linking densities of the PEGylated nanogels were varied from 1 to 5 mol%, and their cytotoxicities were evaluated. The physicochemical characteristics of the pH-sensitive PEGylated nanogels with different cross-linking densities are summarized in Table 1. Although the size of each nanogel at a pH of 7.4 is comparable regardless of the cross-linking density, the swelling ratios of the nanogels (volume ratio at pH values of 5.5 to 7.4) decreased with increasing cross-linking density of the polyamine gel core due to the restriction of the swelling by the highly cross-linked structure. The ζ-potential of all nanogels showed a similar tendency, decreasing with increasing cross-linking density of the polyamine gel core at a pH of 5.5, but having a value of almost zero at pH = 7.4. This result indicates that the dangling polyamine chains from the core network were exposed to the outer shell, whereas at high cross-linking densities they were confined to the core. Thus, PEGylated nanogels with different cross-linking densities were successfully synthesized.

3-2. Effect of cross-linking density of PEGylated nanogels on *in vitro* toxicities

For the evaluation of the cytotoxicity of these nanogels, colon-26 cells were exposed to each nanogel for 24 h and their viability was determined by the WST-8 assay, as shown in Figure 1. The cytotoxicity of the nanogels was remarkably reduced by increasing their cross-linking densities. The value of 50% of inhibitory concentration (IC_{50}) values of nanogels with cross-linking densities of 1, 2, and 5 mol% were determined to be 12, 190, and >1000 μg/mL, respectively. For the further evaluation of the toxicity of the nanogels, their hemolytic activities were evaluated after incubation with RBCs for

1 h (Figure 2). Similar to the results of the cytotoxicity assay, 10% of hemolytic concentration (HC_{10}) values of the nanogels with cross-linking densities of 1, 2, and 5 mol% were determined to be 10, 230, and 700 μg/mL, respectively. Generally, most cationic polymers, including poly(ethylenimine) (PEI) and poly(L-lysin) (PLL), showed high toxicities; this is brought about by the electrostatic interactions between the positively charged polycations and the negatively charged cellular membrane, and the consequent membrane disruption [26]. Thus, these results suggest that highly cross-linked nanogels show negligible contact with cells or RBCs because the high level of cross-linking in the gel structure decreases the exposure of the polyamines, as stated above. It is noteworthy, that the PEGylated nanogels with a cross-linking density of 5 mol% showed negligible toxicities despite the abundance of amino groups in the core maintaining their pH sensitivity.

In order to validate the lowered toxicity of these highly cross-linked nanogels under *in vivo* conditions, we evaluated their acute toxicities via i.v. administration in mice. Figure 3 shows the survival rate of mice after i.v. administration of each nanogel for different injected doses. The median lethal doses (LD_{50}) of nanogels with cross-linking densities of 1, 2, and 5 mol% were determined to be <20, 92, and >200 mg/kg, respectively, meaning that the acute toxicities of the nanogels against mice were significantly reduced by increasing their cross-linking densities. These results are well correlated with the tendencies found for the *in vitro* cytotoxicity and hemolytic activity. It should be noted that the PEGylated nanogels with a cross-linking density of 5 mol% showed significantly higher LD_{50} values than linear PEI (5 mg/kg) and PLL (<30 mg/kg) [27,28]. Thus, increasing the cross-linking densities of the polyamine gel cores of these nanogels is a rational method for reducing both the *in vitro* and *in vivo* toxicities of the amines.

3-3. [^{125}I]-labeling of PEGylated nanogels and biodistribution studies

Since nanogels with low cross-linking density (1 mol% and 2 mol%) showed fairly high acute toxicity *in vivo* within several hours after i.v. administration (Figure 3), these samples were excluded from biodistribution study. Thus pharmacokinetics study was performed only nanogels with a cross-

linking density of 5 mol%. To verify the biodistrubution of systemically administered PEGylated nanogels, we labeled them with radioisotopes. For the biodistribution study, the nanogel containing the *p*-vinylphenol moiety (VP-nanogel) with a cross-linking density of 5 mol% was newly synthesized for the [^{125}I]-labeling, as shown in Scheme 1; PEES was used as a precursor for vinylphenol to avoid the side reaction between the radical species and vinylphenol. After the deprotection of PEES under acidic conditions, the VP-nanogel was successfully obtained without any side reaction. Note that the installation of 5 mol% vinylphenol in the core of the nanogel did not affect the size, swelling ratio, or cytotoxicity (data not shown).

Radiolabeling of the VP-nanogel with [^{125}I] was carried out using the chloramine-T method [19,20], and [^{125}I]-labeling was confirmed by size exclusion chromatography on a PD-10 column (Supporting information, Figure S2). When the PEGylated nanogels containing vinylphenol moieties were reacted with Na[^{125}I] and chloramine-T, almost all the [^{125}I] was labeled to the nanogels, whereas the PEGylated nanogels without vinylphenol could not be labeled with [^{125}I] through this procedure. Additionally, PEGylated nanogels containing non-deprotected PEES moieties could not be labeled with [^{125}I] (data not shown), indicating that the nanogels were selectively labeled with [^{125}I] at the vinylphenol moieties of their cores.

The [^{125}I]-labeled nanogels were injected intravenously in mice at 200 kcpm/mouse, and the concentration of the VP-nanogel in systemic circulation and its major organs (heart, lung, liver, spleen and kidney) were evaluated 5 min, 1 h, and 3 h i.v. injection. One hour after i.v. injection, the concentration of VP-nanogel in the blood was found to be below 1% I.D., and approximately 70% of the VP-nanogel was accumulated in the liver and spleen (Figure 4). The 5 mol% cross-linked nanogel showed a ζ-potential of about zero and fairly low cytotoxicity, as well as low *in vitro* hemolytic concentration as stated above. In the *in vivo* experiments, almost all the nanogel was eliminated from the blood stream within 1 h. This fact means that the recognition level of exogenous synthetic materials under *in vivo* condition might be extremely sensitive compared to that *in vitro* conditions, and only the surface charge shielding and/or hemolytic concentration is not adequate for systemic applications.

Although the ζ-potential of the PEGylated nanogel with 5 mol% cross-linking was close to zero, the living body recognized the internal surface charge of the nanogel. Indeed, PEGylated polyion complexes between PEG-PEI copolymer and siRNA shows short blood circulation time, presumably due to the exogenous recognition arising from their internal positive charge [29, 30]. In order to improve the stealth character of nanogels, an uncompromised surface design must be achieved. In this biodistribution study, PEG macromonomers with relatively high molecular weight (M_n = 9,500) were employed for the nanogel synthesis. However, intravenously administered nanogels were rapidly eliminated from systemic circulation, as shown in Figure 4. We have previously reported the construction of mixed-PEG brush surface which is coimmobilization of long and short PEG chains with different molecular weight to increase PEG density and improve non-fouling character of the substrate surface [31, 32]. In order to improve the surface character, the installation of a short PEG brush on the PEGylated nanogels was examined.

3-4. Biodistribution studies of post-PEGylated nanogels.

We have already confirmed that a density of PEG chain tethered on nanogel surface did not change regardless of the reaction condition due to the steric repulsion of PEG chain. The average PEG chain density was ca. 0.03 chain / nm^2, which is not enough high for anti-biofouling character [33]. From our basic investigation on density of PEG tethered chain on non-specific adsorption of proteins, at least 0.4 chains/nm^2 is required for flat surface [34]. Rounded particle surface requires much more PEG chain density. To increase the PEG density of the nanogels, we carried out post-PEGylation through the Menschutkin reaction between the EAMA moieties in the core of the nanogel and the bromobenzyl-terminated PEG, as shown in Scheme 2. This post-PEGylation technique may also be applied to new methodology for ligand installation using bifunctional PEG. As a control, quaternized polyamine nanogel (QNG) was synthesized through the same procedure, because the EAMA moieties are converted into the quaternized ammonium form by the Menschutkin reaction. In this reaction, short MeO-PEG-Bz-Br (M_n = 500) was employed to construct a mix-PEG tethered chain structure. The

amount of modified PEG was determined by quantifying the residual EAMA by potentiometric titration. The extent of substitution (ES) of EAMA with PEG-Bz-Br at feed [PEG-Bz-Br]/[N] ratios of 0.5 and 5.0 was 64% and 92%, respectively (Table 2). The obtained post-PEGylated nanogels (PNGs) are abbreviated as PNG(64) and PNG(92), respectively, based on their ES of short PEG; PNG(0), PNG(64) and PNG(92) contains 0.9 mol%, 37.1 mol% and 45.8 mol% of total PEG chains (PEG macromonomer + post-modified short PEG), respectively. After [^{125}I]-labeling, the blood circulation time and body disposition of systemically administered PNG were investigated, and it was found that the insertion of shorter PEG chains extended the blood circulation time of the nanogels (Figure 5). The % I.D. of PNG(64) and PNG(92) 1 h after i.v. administration in the blood was 2% I.D. and 7% I.D., respectively, clearly showing that the blood circulation time of the nanogels was prolonged as the ES of the underlayered PEG increased. There are several reports on prolonged blood circulation of nanoparticles such as PEGylated liposomes and polymer micelles. For example, block copolymer micelle composed of peptide-PEG-*b*-poly(D,L-lactide) showed fairly long circulating character (20% of injected dose retained in blood stream after 24 h) [35]. In the present nanogel system, however, post-PEGylation was carried out via Menschutkin reaction, which introduced fixed cationic charge in the core. In spite of the increase in fixed positive charge, the blood circulation of PNG(94) increased to 7% I.D., indicating strong entropically shielding effect of PEG layer owing to the increase in its density by the post-PEGylation reaction. To further confirm the contribution of this underlayered PEG, the blood circulation time of QNG was investigated. However, the quaternized amines in the core of the nanogel did not affect the blood circulation time, with QNG showing blood circulation similar to the case of unmodified nanogels (Figure 5a). To verify the prolonged blood circulation time of the nanogels, their accumulation in major tissues was investigated. The body distributions of PNG(64) and PNG(92) are shown in Figure 5b; the liver accumulation was significantly decreased by the installation of quaternary amines, while the lung accumulation was increased as compared to PNG(0). The lung accumulation of QNG was of the same level PNG(64) and PNG(92) (Figure 5). Therefore, the increased lung accumulation observed for systemically administered PNG was presumably due to the effect of the

15

quaternary amine moieties. Although decrease in lung accumulation of PNG(92) is slight compared to that of PNG(64), definite difference was observed ($p < 0.05$), indicating that increase in the PEG chain density on particle surface suppresses non-specific entrapment in reticuloendothelial system in lung. These biodistribution results suggest that the prolonged blood circulation time observed for PNG was mainly because of the increase in surface PEG density with the mix-PEG tethered chain structure, and not a result of the contribution of the quaternary amino groups. In this study, short PEG ($M_n = 500$) was utilized as the underlayer PEG for post-PEGylation. Despite its prolonged blood circulation, the use of PNG is still controversial due to its rapid diffusion throughout the body, especially in major organs such as liver, spleen, and lung. The rapid diffusion of drug carriers in these tissues causes the decrease in the therapeutic effect on targeted tissue (e.g. tumor tissue), as well as increase the severity of side effects. The lung accumulation of PNG might be reduced when longer PEG is employed for further post-PEGylation. Further investigations are now in progress and will be published elsewhere.

Conclusion

The impact of different cross-linking densities nanogel cores on their toxicity was determined. When the cross-linking density of the nanogels was increased, the nanogels showed negligible *in vitro* and *in vivo* toxicities, despite the abundance of amino groups in the core. Accordingly, the LD_{50} values of nanogels with a cross-linking density of 5 mol% were greater than 200 mg/kg. The body disposition study of PEGylated nanogels revealed that intravenously administered nanogels were rapidly eliminated from the blood, even though their size was below 100 nm and ζ-potential measurements showed a neutral surface charge. Thus, the *in vitro* physicochemical characteristics of PEGylated nanogels seem to be insufficient for estimating the *in vivo* biodistribution. To improve the blood circulation time, surface PEG density of nanogels were further increased by post-PEGylated reaction by Menschutkin reaction using bromobenzyl-terminated short PEG. The blood circulation time of thus synthesized post-PEGylated nanogels was prolonged as the short PEG content increased. The % I.D. of post-PEGylated nanogel, with 92% of the extent of substitution of EAMA moieties in the nanogels with PEG-Bz-Br, was about seven times higher than that of nanogels without post-PEGylation. In spite of the increase in fixed positive charge by the Menschutkin reaction with short PEG-Bz-Br, the blood circulation of PNG(94) increased to 7% I.D., indicating strong entropically shielding effect of PEG layer owing to the increase in its density by the post-PEGylation reaction. Thus, PEG chain density on the surface of nanoparticle primarily works to improve their blood circulation character. Several other methods to increase in PEG shell layer are now in progress in our group and will be published elsewhere.

References

1. Cho K, Wang X, Nie S, Chen ZG, Shin DM. Therapeutic Nanoparticles for Drug Delivery in Cancer. Clinical Cancer Research 2008;14(5):1310-1316.

2. Kabanov AV. Polymer genomics: an insight into pharmacology and toxicology of nanomedicines. Advanced drug delivery reviews 2006;58(15):1597-1621.

3. Davis ME, Chen ZG, Shin DM. Nanoparticle therapeutics: an emerging treatment modality for cancer. Nature Reviews Drug Discovery 2008;7(9):771–782.

4. Harris JM, Chess RB. Effect of PEGylation on pharmaceuticals. Nature Reviews Drug Discovery 2003;2(3):214-221.

5. Kwon G, Kataoka K. Block copolymer micelles as long-circulating drug vehicles. Advanced Drug Delivery Reviews 1995;16(2-3):295-309.

6. Lee M, Kim SW. Polyethylene Glycol-Conjugated Copolymers for Plasmid DNA Delivery. Pharmaceutical Research 2005;22(1):1-10.

7. Maeda H, Wu J, Sawa T, Matsumura Y, Hori K. Tumor vascular permeability and the EPR effect in macromolecular therapeutics: a review. Journal of controlled release 2000;65:271-284.

8. Oh J, Drumright R, Siegwart D, Matyjaszewski K. The development of microgels/nanogels for drug delivery applications. Progress in Polymer Science 2008;33(4):448-477.

9. Ganta S, Devalapally H, Shahiwala A, Amiji M. A review of stimuli-responsive nanocarriers for drug and gene delivery. Journal of Controlled Release 2008;126:187-204.

10. Hoffman AS, Stayton PS. Conjugates of stimuli-responsive polymers and proteins. Progress in Polymer Science 2007;32(8):922-932.

11. Immordino ML, Dosio L, Cattel L. Stealth liposomes : review of the basic science, rationale, and clinical applications, existing and potential. International Journal of Nanomedicine 2006;297-315.

12. Torchilin VP. Structure and design of polymeric surfactant-based drug delivery systems. Journal of Controlled Release 2001;73:137-172.

13. Hayashi H, Iijima M, Kataoka K, Nagasaki Y. pH-Sensitive Nanogel Possessing Reactive PEG Tethered Chains on the Surface. Macromolecules 2004;37(14):5389-5396.

14. Oishi M, Nagasaki Y. Stimuli-responsive smart nanogels for cancer diagnostics and therapy. Nanomedicine 2010;5(3):451-468.

15. Oishi M, Hayashi H, Iijima M, Nagasaki Y. Endosomal release and intracellular delivery of anticancer drugs using pH-sensitive PEGylated nanogels. Journal of Materials Chemistry 2007;17(35):3720.

16. Nakamura T, Tamura A, Murotani H, Oishi M, Jinji Y, Matsuishi K, Nagasaki Y. Large payloads of gold nanoparticles into the polyamine network core of stimuli-responsive PEGylated nanogels for selective and noninvasive cancer photothermal therapy. Nanoscale 2010;2(5):739-746.

17. Tamura A, Oishi M, Nagasaki Y. Enhanced cytoplasmic delivery of siRNA using a stabilized polyion complex based on PEGylated nanogels with a cross-linked polyamine structure. Biomacromolecules 2009;10(7):1818–1827.

18. Tamura A, Oishi M, Nagasaki Y. Efficient siRNA delivery based on PEGylated and partially quaternized polyamine nanogels: enhanced gene silencing activity by the cooperative effect of tertiary and quaternary amino groups in the core. Journal of controlled release 2010;146(3):378-387.

19. Greenwood FC, Hunter WM, Glover JS. The preparation of ^{131}I-labeled human growth hormone of high specific radioactivity. The Biochemical journal 1963;89(1):114-123.

20. Almutairi A, Rossin R, Shokeen M, Hagooly A, Ananth A, Capoccia B, Guillaudeu S, Abendschein D, Anderson CJ, Welch MJ, Fréchet JM. Biodegradable dendritic positron-emitting nanoprobes for the noninvasive imaging of angiogenesis. Proceedings of the National Academy of Sciences of the United States of America 2009;106(3):685-690.

21. Glos M, Reiser O. Aza-bis(oxazolines): new chiral ligands for asymmetric catalysis. Organic letters 2000;2(14):2045-2048.

22. Bütün V, Armes SP, Billingham NC. Selective Quaternization of 2-(Dimethylamino)ethyl Methacrylate Residues in Tertiary Amine Methacrylate Diblock Copolymers. Macromolecules 2001;34(5):1148-1159.

23. Ishiyama M, Miyazono Y, Sasamoto K, Ohkura Y, Ueno K. A highly water-soluble disulfonated tetrazolium salt as a chromogenic indicator for NADH as well as cell viability. Talanta 1997;44(7):1299-1305.

24. Fischer D, Li Y, Ahlemeyer B, Krieglstein J, Kissel T. *In vitro* cytotoxicity testing of polycations: influence of polymer structure on cell viability and hemolysis. Biomaterials 2003;24(7):1121-1131.

25. Oishi M, Hayashi H, Itaka K, Kataoka K, Nagasaki Y. pH-Responsive PEGylated nanogels as targetable and low invasive endosomolytic agents to induce the enhanced transfection efficiency of nonviral gene vectors. Colloid and Polymer Science 2007;285(9):1055-1060.

26. Choksakulnimitr S, Masuda S, Tokuda H, Takakura Y, Hashida M. *In vitro* cytotoxicity of macromolecules in different cell culture systems. Journal of Controlled Release. 1995;34:233-241.

27. Di Stefano G, Busi C, Mattioli A, Fiume L. Selective delivery to the liver of antiviral nucleoside analogs coupled to a high molecular mass lactosaminated poly-L-lysine and administered to mice by intramuscular route. Biochemical Pharmacology 1995;49(12):1769-1775.

28. Chollet P, Favrot MC, Hurbin A, Coll J-L. Side-effects of a systemic injection of linear polyethylenimine-DNA complexes. The journal of gene medicine 2002;4(1):84-91.

29. Bartlett DW, Su H, Hildebrandt IJ, Weber WA, Davis ME. Impact of tumor-specific targeting on the biodistribution and efficacy of siRNA nanoparticles measured by multimodality *in vivo* imaging. Proceedings of the National Academy of Sciences of the United States of America 2007;104(39):15549-15554.

30. Malek A, Merkel O, Fink L, Czubayko F, Kissel T, Aigner A. *In vivo* pharmacokinetics, tissue distribution and underlying mechanisms of various PEI(-PEG)/siRNA complexes. Toxicology and applied pharmacology 2009;236(1):97-108.

31. Uchida K, Hoshino Y, Tamura A, Yoshimoto K, Kojima S, Yamashita K, Yamanaka I, Otsuka H, Kataoka K, Nagasaki Y. Creation of a mixed poly(ethylene glycol) tethered-chain surface for preventing the nonspecific adsorption of proteins and peptides. Biointerphases 2007;2(4):126-130.

32. Yuan X, Yoshimoto K, Nagasaki Y. High-performance immunolatex possessing a mixed-PEG/antibody coimmobilized surface: highly sensitive ferritin immunodiagnostics. Analytical chemistry 2009;81(4):1549-1556.

33. Ogawa R, Nagasaki Y, Shibata N, Otsuka H, Kataoka K. Core-Shell Type Polystyrene Latex Possessing Reactive Poly(ethylene glycol) Brushes on the Surface for High Performance Immunodiagnostics. Polymer Journal 2002;34(12):868-875.

34. Uchida K, Otsuka H, Kaneko M, Kataoka K, Nagasaki Y. A reactive poly(ethylene glycol) layer to achieve specific surface plasmon resonance sensing with a high S/N ratio: the substantial role of a short underbrushed PEG layer in minimizing nonspecific adsorption. Analytical chemistry 2005;77(4):1075-1080.

35. Yamamoto Y, Nagasaki Y, Kato Y, Sugiyama Y, Kataoka K. Long-circulating poly(ethylene glycol)-poly(D,L-lactide) block copolymer micelles with modulated surface charge. Journal of controlled release 2001;77(1-2):27-38.

Tables

Table 1. The sizes and ζ-potentials of PEGylated nanogels with different cross-linking densities

feed EGDMA (mol%)	size (nm)*1		ζ-potential (mV)*2		swelling ratio*3
	pH = 5.5	pH = 7.4	pH = 5.5	pH = 7.4	
1	141	97	6.4	0.3	3.2
2	115	93	3.4	0.03	2.0
5	116	103	0.6	0.1	1.4

*1 As determined by DLS in phosphate buffer (10 mM PB, 150 mM NaCl) at 37 °C

*2 As determined by electrophoretic light scattering in phosphate buffer (10m M PB) at 37 °C

*3 The swelling ratio of nanogel is defined as the volume ratio at pH = 5.5/pH = 7.4

Table 2. Characterization of nanogels reacted with bromobenzyl-terminated short PEG

feed [MeO-PEG-Bz-Br]/[EAMA] ratio (mol/mol)	size (nm)*1		ζ-potential (mV)*2		Swelling ratio*3	ES (%)*4
	pH = 5.5	pH = 7.4	pH = 5.5	pH = 7.4		
0	91	73	2.7	0.6	1.9	0
0.5	104	99	- 0.1	0.1	1.2	64
5.0	109	108	0.0	0.1	1.0	92

*1 As determined by DLS in phosphate buffer (10 mM PB, 150 mM NaCl) at 37 °C

*2 As determined by electrophoretic light scattering in phosphate buffer (PB 10 mM) at 37 °C

*3 The swelling ratio of nanogel is defined as the volume ratio at pH = 5.5/pH = 7.4

*4 ES = extent of substitution of EAMA with MeO-PEG-Bz-Br (M_n = 500) determined by potentiometric titration
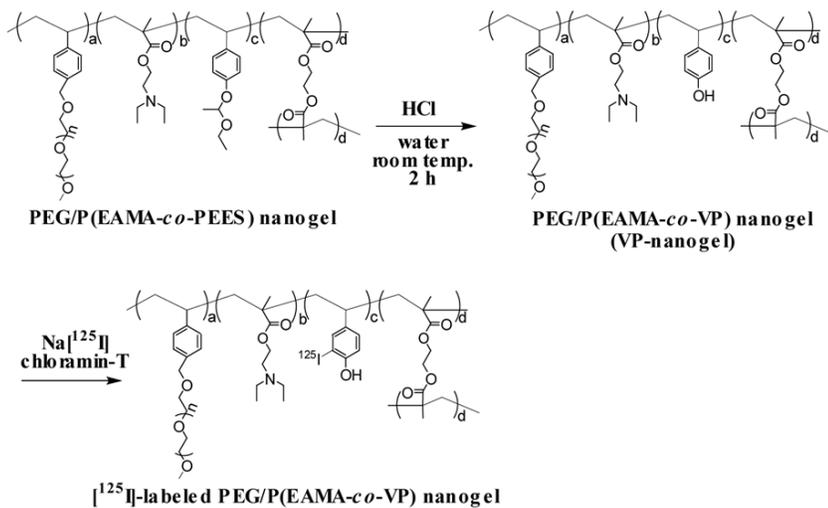
Scheme 1. [125I]-labeling of PEGylated nanogel containing vinylphenols by the chloramine-T method
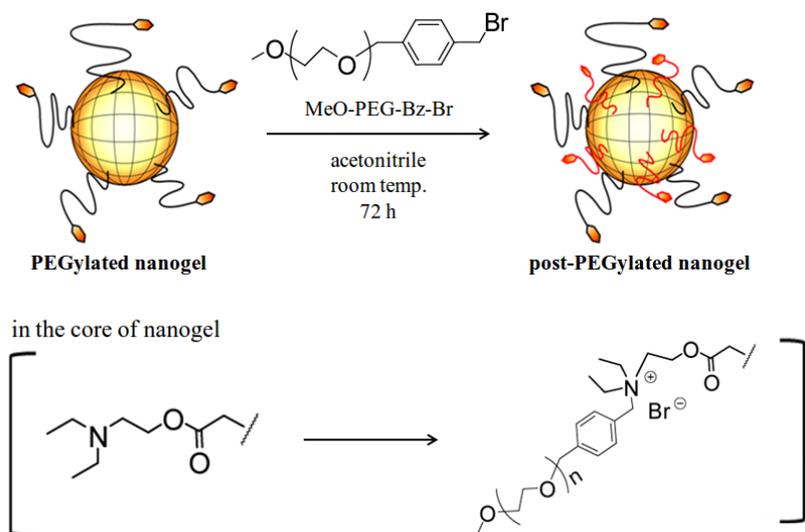
Scheme 2. Synthesis of post-PEGylated nanogels by the Menschutkin reaction with bromobenzyl-terminated short PEG

Figure captions

Figure 1. Cytotoxicities of PEGylated nanogels with different cross-linking densities against colon-26 cells, as determined by the WST-8 assay after 24 h incubation. The plots represent PEGylated nanogels with cross-linking densities of 1 mol% (closed squares), 2 mol% (closed triangles), and 5 mol% (open circles). The data are expressed as mean ± S.D. (n = 6).

Figure 2. Hemolytic activities of PEGylated nanogels with different cross-linking densities against 1×10^7 RBCs after 1 h incubation. The plots represent PEGylated nanogels with cross-linking densities of 1 mol% (closed squares), 2 mol% (closed triangles), and 5 mol% (open circles). The data are expressed as mean ± S.D. (n = 3).

Figure 3. Survival rate of ICR mice 24 h after i.v. administration of PEGylated nanogels with different cross-linking densities. The plots represent PEGylated nanogels with cross-linking densities of 1 mol% (closed squares), 2 mol% (closed triangles), and 5 mol% (open circles). (n = 5–8).

Figure 4. The biodistribution of [^{125}I]-labeled nanogels with a cross-linking density of 5 mol% (a) Time course of % I.D. of [^{125}I]-labeled nanogels in the blood after i.v. administration. (b) Body disposition of [^{125}I]-labeled nanogels 1 h after i.v. administration. The data are expressed as mean ± S.D. (n = 4).

Figure 5. The difference in biodistribution of post-PEGylated [^{125}I]-labeled nanogels with a cross-linking density of 5 mol% (a) Time course of % I.D. of [^{125}I]-labeled nanogels with different degrees of short PEG substitution and 98% CH$_3$I substitution (QNG) in the blood after i.v. administration. (b) Body disposition of [^{125}I]-labeled nanogels with different short PEG and QNG 1 h after i.v. administration. The plots and bars represent the PEGylated nanogels with different degrees of PEG-Bz-Br substitution 0 (black symbols), 64 (cancellous symbols), and 92 mol% (dot symbols) and for a CH$_3$I

substitution degree of 98% (diagonal symbols). The data is expressed as mean ± S.D. (n = 4). *$p < 0.05$

significantly different from nanogel with ES% = 0 by one-way ANOVA with Student's *t*-test.

Figure 1

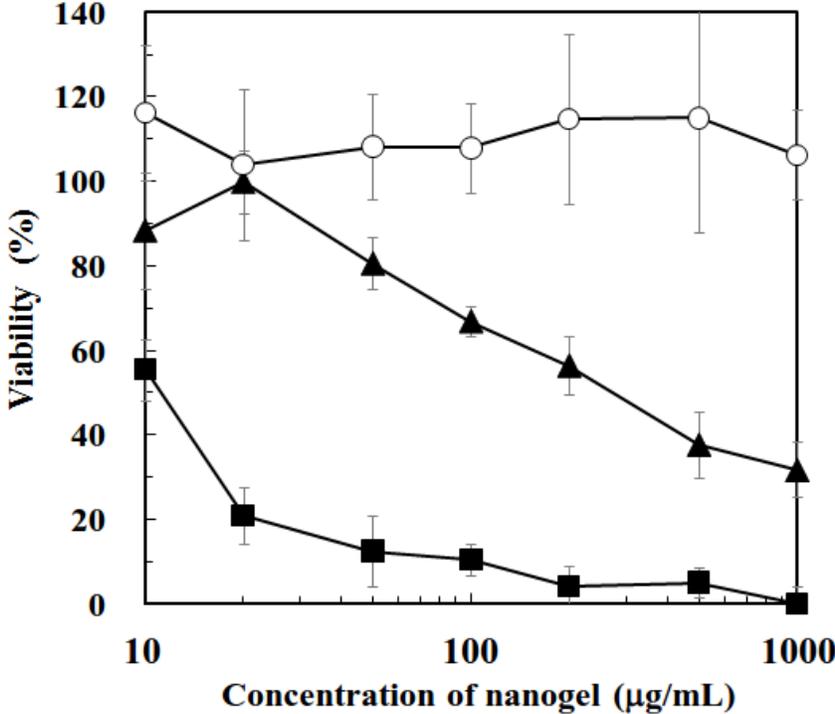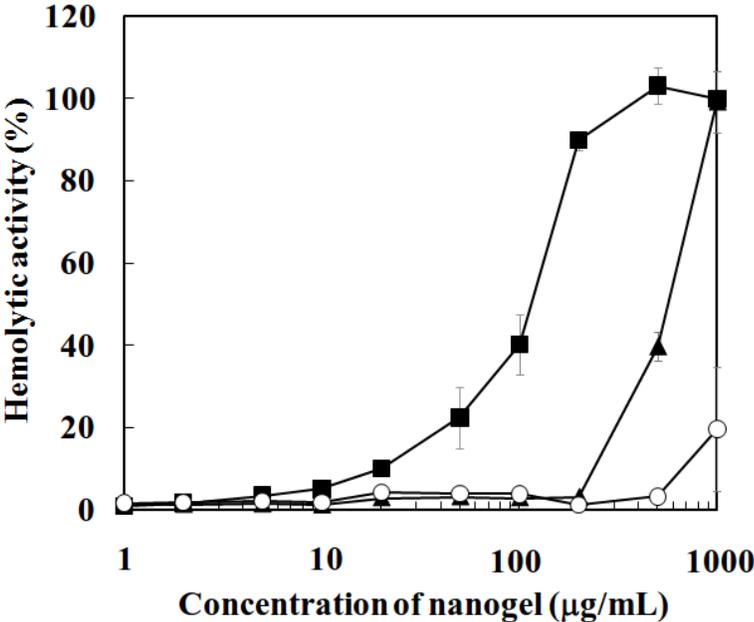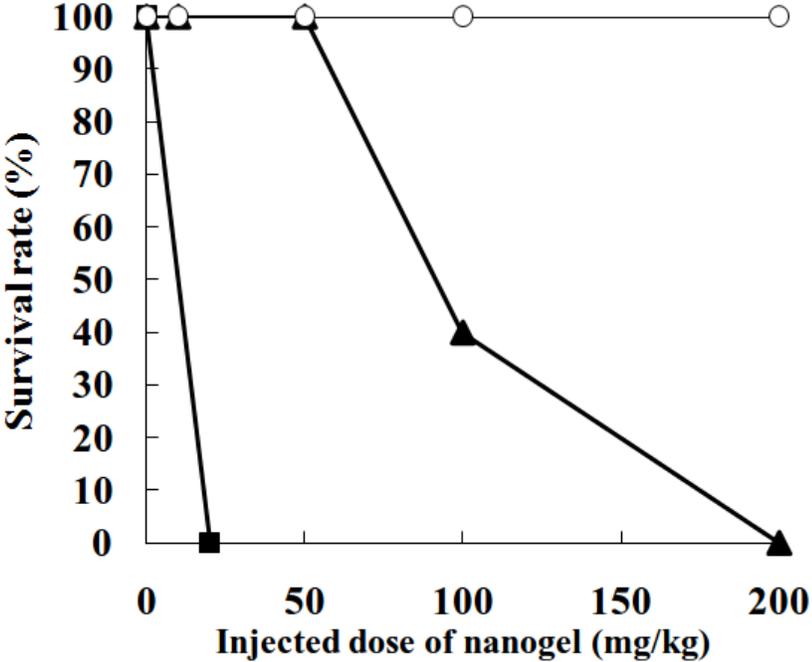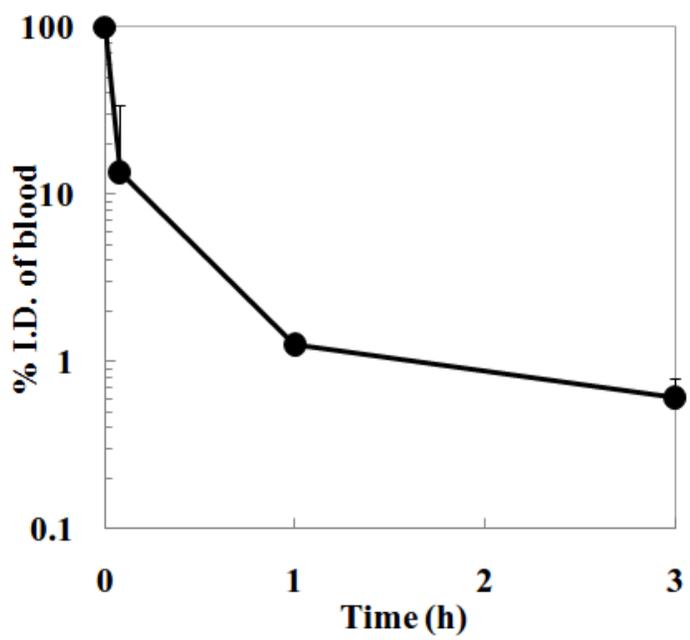**Figure 2**

Figure 3

Figure 4

(a)

(b)
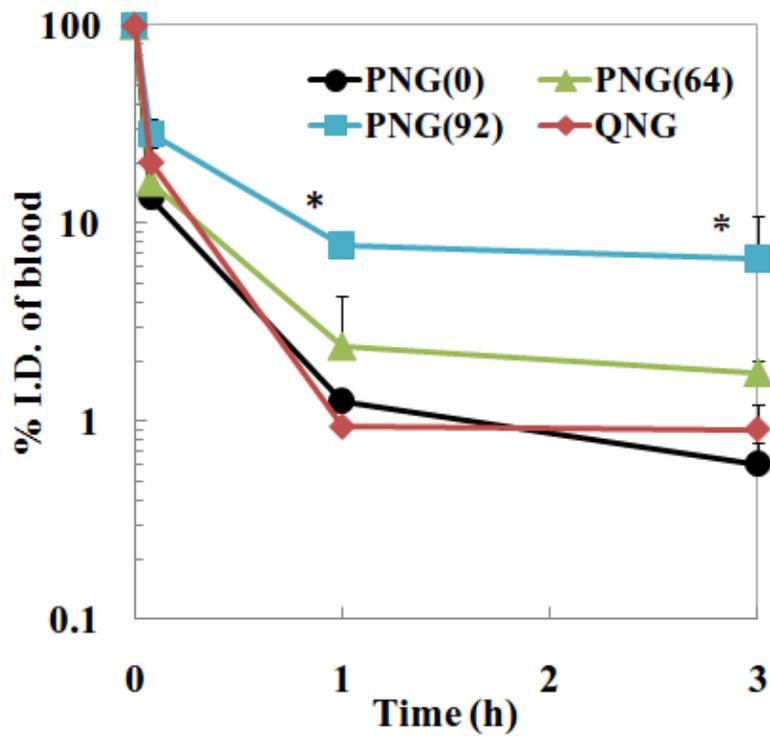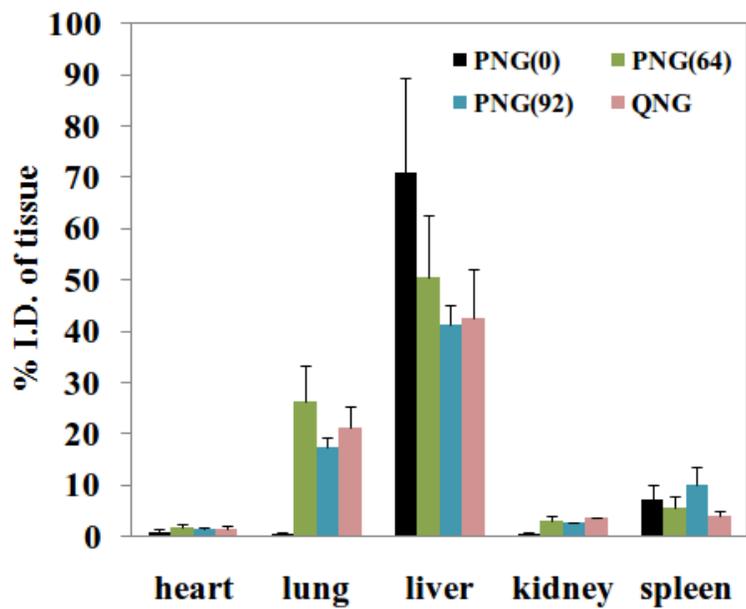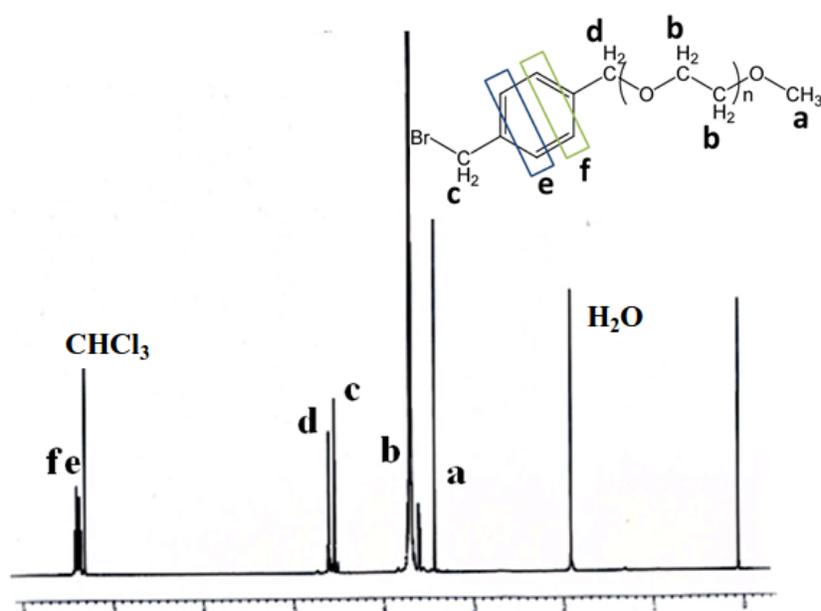
Figure 5

(a)

(b)

In Vitro and In Vivo Characteristics of Core–Shell-Type Nanogel Particles: Optimization of Core Cross-Linking Density and Surface PEG Density in PEGylated Nanogels

Masato Tamura[1], Satoshi Ichinohe[2], Atsushi Tamura[2], Yutaka Ikeda[2,3,4], and Yukio Nagasaki[1,2,3,4,5,*]

[1]Graduate School of Comprehensive Human Sciences, University of Tsukuba, 1-1-1 Ten-noudai, Tsukuba, Ibaraki 305-8573, Japan. [2]Graduate School of Pure and Applied Sciences, University of Tsukuba, 1-1-1 Ten-noudai, Tsukuba, Ibaraki 305-8573, Japan. [3]Tsukuba Research Center for Interdisciplinary Materials Science (TIMS), University of Tsukuba, 1-1-1 Ten-noudai, Tsukuba, Ibaraki 305-8573, Japan. [4]Center for Tsukuba Advanced Research Alliance (TARA), University of Tsukuba, 1-1-1 Ten-noudai, Tsukuba, Ibaraki 305-8573, Japan. [5]International Center for Materials Nanoarchitectonics Satellite (MANA), National Institute for Materials Science (NIMS) and University of Tsukuba 1-1-1 Ten-noudai, Tsukuba, Ibaraki 305-8573, Japan

* Corresponding author. Prof. Yukio Nagasaki (Tel: +81-29-853-5749. Fax: +81-29-853-5749. E-mail: yukio@nagalabo.jp).

Figure S1. ^{1}H-NMR chart of MeO-PEG-Bz-Br in CDCl$_3$. The integration values were follows: Peak a = 2.95H, b =52H, c = 1.93H, d = 1.94H, e = 1.82H and f = 1.82H.
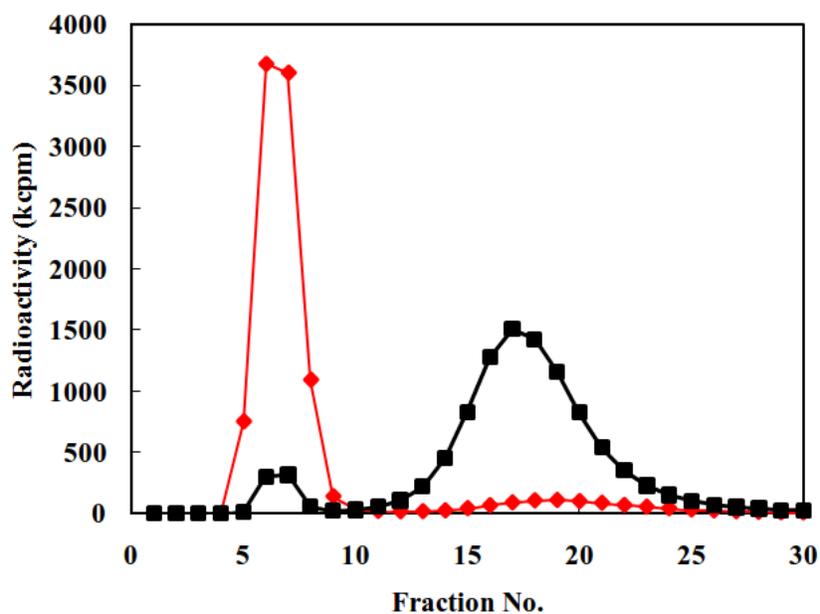
Figure S2. Size exclusion chromatograms of PEGylated nanogel bearing vinylphenol moieties in the core (closed lozenges) and control nanogels without vinylphenol moieties (closed squares) after reaction with Na[^{125}I], detected by γ-counter.